Biophysical Journal Volume 67 August 1994 706–712

Freezing and Melting Water in Lamellar Structures

J. T. Gleeson, Shyamsunder Erramilli, and S. M. Gruner
Department of Physics, Joseph Henry Laboratories, Princeton University, Princeton, New Jersey 08544 USA

ABSTRACT The manner in which ice forms in lamellar suspensions of dielaidoylphosphatidylethanolamine, dielaidoylphosphatidylcholine, and dioleoylphosphatidylcholine in water depends strongly on the water fraction. For weight fractions between 15 and 9%, the freezing and melting temperatures are significantly depressed below 0°C. The ice exhibits a continuous melting transition spanning as much as 20°C. When the water weight fraction is below 9%, ice never forms at temperatures as low as −40°C. We show that when water contained in a lamellar lipid suspension freezes, the ice is not found between the bilayers; it exists as pools of crystalline ice in equilibrium with the bound water associated with the polar lipid headgroups. We have used this effect, together with the known chemical potential of ice, to measure hydration forces between lipid bilayers. We find exponentially decaying hydration repulsion when the bilayers are less than about 7 Å apart. For larger separations, we find significant deviations from single exponential decay.

INTRODUCTION

Water is the most ubiquitous and the most important biological molecule. A copious quantity of research has been devoted to the study of water's effect on diverse biophysical and biochemical systems including, but not limited to, proteins (Zimmerberg and Parsegian, 1986, Colombo et al., 1992), DNA (Rau and Parsegian, 1992), and lipids (Kodama et al., 1987). Comparatively little work has been devoted to the effect of a biological "substrate" on water itself, although there is a considerable body of work on so-called "antifreeze" peptides (Knight and DeVries, 1989; Knight et al., 1991), as well as calorimetric indications of glassy water in protein systems (Doster et al., 1986).

Using x-ray diffraction, we have examined the behavior of water incorporated into lipid bilayers as it is cooled well below the normal freezing point of water. Biologically, these questions have considerable practical importance, especially from the point of view of organism cryoprotection. Indeed, there are indications that the presence of the cell membrane plays an important role in the winter-hardiness of trees (Hirsh et al., 1985).

The issue is also of fundamental physical importance. Such basic properties of water as the density (Narayan et al., 1990) and the dielectric constant (Singh et al., 1981) are known to be altered by the hydrophilic moieties on either lipid headgroups or globular proteins. How do these solvent-solute interactions affect ice formation? Furthermore, one characteristic of various polymorphic lipid-water phases is that water is confined in channels of microscopic dimension; different lipid morphologies confine the water in one, two, or three dimensions. How does this confinement affect the freezing behavior of water? The effect of confinement on phase transitions is a mature subject. Basically, the Kelvin equation relates the change in transition temperature of a system confined in one dimension within distance d with respect to the infinite system:

$$\frac{T_\infty - T_d}{T_\infty} = \frac{2\gamma}{Ld} \tag{1}$$

T_∞ is the transition temperature in an infinite system, and T_d is the transition temperature observed in the confined system. γ is the surface energy between the two phases, and L is the latent heat/unit volume of the transition. The quantity γ/L is the capillary length d_c. For the freezing of water, $d_c < 1$ Å. Right away, one must be careful in applying equilibrium thermodynamics, on which the Kelvin equation is based, when a relevant length scale is smaller than the constituent molecules.

MATERIALS AND METHODS

Dielaidoylphosphatidylethanolamine (DEPE), dielaidylphosphatidylcholine (DEPC), and dioleoylphosphatidylcholine (DOPC) were all purchased from Avanti Polar Lipids (Birmingham, AL) and used without further purification. For each sample, a quantity of lipid was weighed into an x-ray capillary. Deionized water was added using a micropipettor, and the water weight fraction was determined gravimetrically. The capillary was then flame-sealed; care was taken to leave an empty space for co-existing water vapor with the flame being applied only some distance away from the lipid-water mixture. Excess water samples were mixed mechanically with the micropipettor; limited water samples were mixed by repeatedly cycling their temperature through the liquid crystal-gel transition.

In as much as we are interested in the melting and freezing behavior of water, precise temperature control is essential. The x-ray capillary containing the sample was held in a thermostated jacket. The jacket was both cooled and heated by thermoelectric elements and the temperature monitored and controlled by a dedicated microcomputer. This setup enabled us to control the temperature to within ±0.02°C; the absolute temperature was accurate to about ±0.5°C.

The main experimental technique used was x-ray diffraction. We used Ni-filtered Cu K_α radiation (wavelength $\lambda = 1.54$ Å), focused and monochromatized with an orthogonal set of Franks mirrors (Milch, 1983). The beam is defined by tantalum slits to be about 200 × 500 μm. The diffracted x rays are collected using a two-dimensional, integrating detector (Gruner, 1989). With small-angle diffraction we can use a range of scattering vectors

---

Received for publication 8 July 1993 and in final form 24 May 1994.

Address reprint requests to J. T. Gleeson at his present address, Department of Physics and Astronomy, The University of Calgary, Alberta, T2N 1N4 Canada. Tel.: 403-220-5413; Fax: 403-289-3331; E-mail: gleeson@acs.ucalgary.ca.

0006-3495/94/08/706/07 $2.00

$q = 4\pi \sin(\theta)/\lambda$, where 2θ is the scattering angle, between about 0.05 Å^{-1} and 0.5 Å^{-1}. An example of an azimuthal integration of the intensity of x rays as a function of scattering vector q is shown in Fig. 1. With wide-angle diffraction we use scattering vectors between 0.5 and 2 Å^{-1}. During the course of this work, it became clear that a wider dynamic range in q would be necessary for some experiments. For this reason, the aperture of the SIT x-ray detector (Gruner et al., 1982) was expanded to 57 mm, enabling it simultaneously to detect scattering vectors between about 0.09 and 1.9 Å^{-1}.

RESULTS

Small angle x-ray diffraction

Small-angle x-ray diffraction studies of the lamellar structure formed by DEPE in excess water show a number of interesting features (Fig. 2). At 20°C, the lattice constant, a, is 65.66 ± 0.05 Å. As the temperature is reduced, a increases very gradually: $da/dT \approx -0.01$ Å/°C. At $T \approx -12.5$°C, a drops precipitously by 3.1 Å. (The degree to which water can be supercooled varies from run to run. This is not unexpected because of the metastable nature of supercooled water. The temperature at which nucleation occurs is observed to vary within a few degrees. There is, however, a definite trend toward greater supercooling as the weight fraction of water is decreased.) Below this temperature, a decreases with decreasing temperature, but not linearly. If the temperature is now raised, a increases with the same dependence on temperature as previously observed until we reach the temperature at which the precipitous drop was observed during cooling. At this point the heating curve deviates from the cooling curve, and a large hysteresis in temperature is observed. Only at 0°C do the two curves again match up, closing the hysteresis loop. It should be noted that the observed hysteresis is not caused by kinetic effects. The shape of the hysteresis curve does not depend on the rate of cooling or heating. Indeed, we have held an excess water sample for more than 6 h at −10°C without seeing the lattice constant drop.

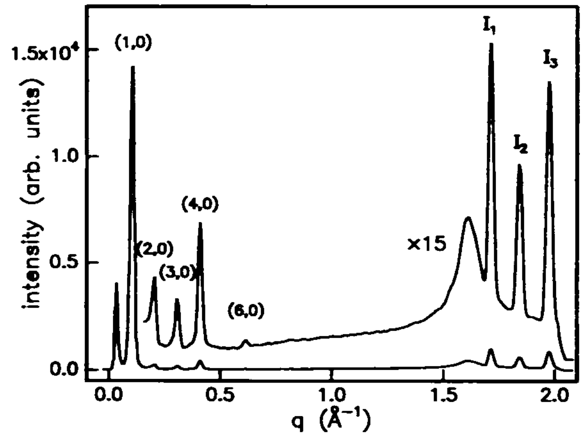

FIGURE 1 Azimuthal integration of x-ray intensity as a function of scattering vector q. This pattern corresponds to DEPC with excess water at −30°C. The lattice constant is 62.25 Å. The Bragg peaks are indexed onto a one-dimensional lattice; the (5,0) peak is canceled by the structure factor. Incoherent scatter around the beam stop is seen at lower q than the (1,0) peak. The three peaks labeled I_1, I_2, and I_3 are the first three Bragg peaks of crystalline ice. Given that the x-ray detector has been calibrated over the small-angle region, the ice peaks appear to be slightly shifted (about 8%) from their true positions. When a wide-angle calibrant is used, the ice peaks are found at the accepted q of ordinary ice. The broad peak at slightly lower q is from the hydrocarbon chains on the lipid.

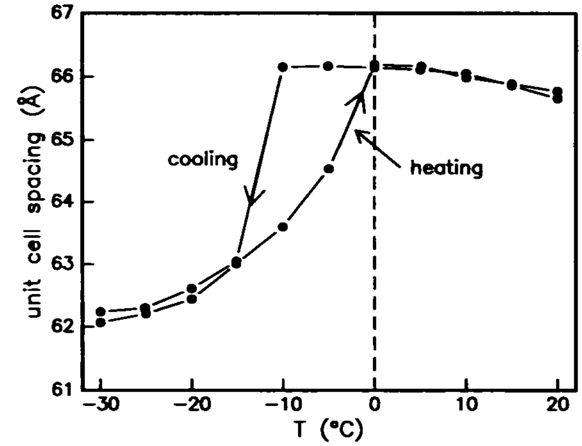

FIGURE 2 Unit cell spacing (a) of DEPE in excess water as a function of temperature. The cooling and heating branches exhibit dramatically different lattice constants between −15°C and 0°C.

If the water fraction is reduced below excess, the same qualitative behavior is observed, but the temperature at which a drops on cooling and the temperature at which the hysteresis loop closes on heating are both lower than in the excess water case. When the water fraction is reduced below about 11 ± 1 wt % no hysteresis in the unit cell spacing is observed for temperatures above −40°C.

The most important feature of these measurements becomes clear when the lattice constants of samples having widely varying water contents are compared. Fig. 3 shows a versus T for a variety of weight fractions of water in DEPE. Consider the curves corresponding to both excess water conditions and water fraction 12.4 wt %. Note that during heating, between −30 and −5°C these two lipid suspensions

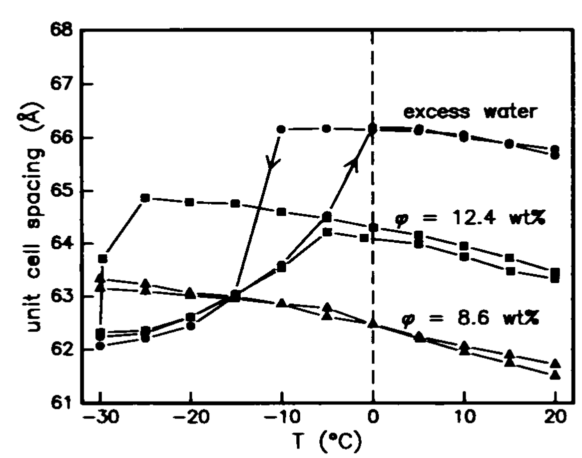

FIGURE 3 Unit cell spacing of DEPE versus temperature for various weight fractions of water as labeled. Note that the curves labeled excess water and $\phi = 12.4$ wt % have the same unit cell spacing when heated from −30°C to −5°C. Also, the sample with $\phi = 8.6$ wt % has a larger unit cell spacing than either of the others between −30°C and −15°C.

have the *same* lattice constant, even though the excess water sample contains about five times as much water. Moreover, and more importantly, the lipid with 8.6 wt % water, which exhibits no hysteresis, has a larger *lattice* constant in the temperature range between −30 and −15°C than either of the two samples that exhibit hysteresis.

Wide-angle x-ray diffraction

Crystalline ice has Bragg peaks at scattering vectors q = 1.605 Å^{-1}, 1.706 Å^{-1}, and 1.817 Å^{-1} (Hodgman, 1952). We monitored the intensity (and indeed the presence) of x rays diffracted with these scattering vectors (see Fig. 1) as indications of ice in the diffracting volume. Fig. 4 shows the intensity of the Bragg peaks characteristic of ice as a function of temperature during both cooling and warming. These data are for DEPE in excess water conditions. The first and most striking observation is the large hysteresis in the intensity of x rays diffracted by ice. This is because on cooling, the water supercooled significantly below 0°C before freezing. We expect that were it possible to prevent supercooling, no hysteresis would be observed. Also notable in this figure is the abrupt disappearance, upon heating, of these Bragg peaks at 0°C. For pure water, melting must occur at a single temperature; as these are excess water conditions, this is expected. Fig. 5 shows the intensity of x rays diffracted by ice for 12.4 wt % water fraction in DEPE. The hysteresis is seen as before, but the curve is both qualitatively and quantitatively different from the excess water situation. First, the supercooling persists to around −30°C. Second, the diffraction has disappeared altogether at about −5°C on warming, not 0°C as before. Third, the x-ray intensity diminishes continuously and smoothly upon warming, in contrast to the excess water case. This indicates that the ice-melting transition occurs over a much *broader* range of temperature than in the excess water case. To complete the story, DEPE with 8.6 wt % water shows no diffraction characteristic of ice for temperatures as low as −40°C.

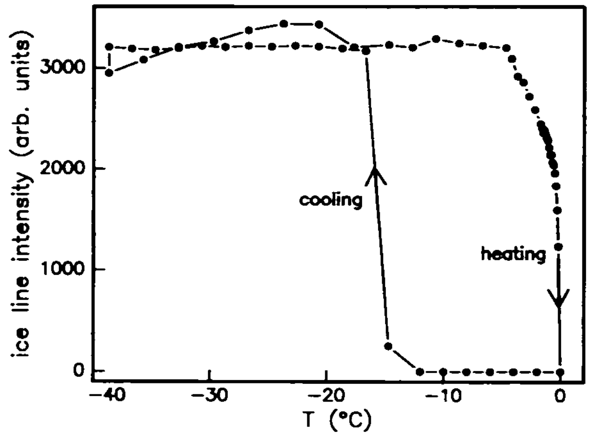

FIGURE 4 Intensity of x rays scattered into the Bragg peaks characteristic of crystalline ice as a function of temperature. The hysteresis here is caused by water supercooling significantly below 0. This curve corresponds to DEPE in excess water. The melting transition here is about 4°C wide, and melting is complete at 0°C.

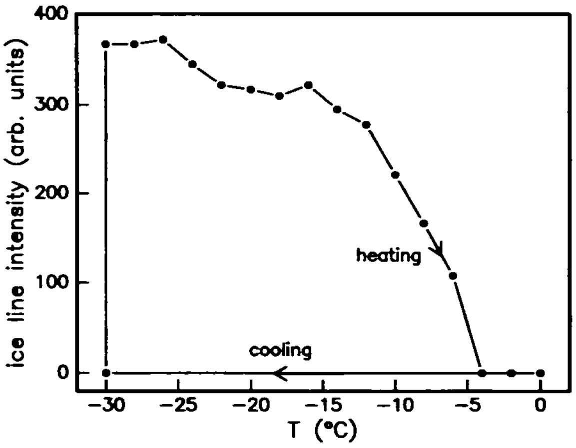

FIGURE 5 Intensity of x rays scattered into the Bragg peaks characteristic of crystalline ice as a function of temperature. This is obtained with 12.4 wt % water in DEPE. Here, the water supercools all the way to −30°C before freezing. In contrast to Fig. 4, the melting has a width over perhaps 20°C. Also, it is completely melted at about −5°C.

Comparing simultaneous small- and wide-angle x-ray diffraction measurements makes one fact abundantly clear. Hysteresis in the lamellar lattice constant as a function of temperature is always accompanied by hysteresis in the intensity of x rays diffracted by ice. Moreover, hysteresis in the lamellar lattice constant is only seen in the temperature range inside which ice is observed. The large drop in the lamellar lattice constant on cooling is always concomitant with the abrupt appearance of ice Bragg peaks. The temperature at which ice diffraction disappears altogether on heating is the temperature at which the cooling and heating values of the lamellar lattice constant are the same. There is one qualitative difference in this comparison. Under excess water conditions, the intensity of x rays diffracted by ice vanishes suddenly at 0°C, whereas the lamellar lattice constant smoothly increases on warming until the hysteresis loop is closed (cf. Figs. 2 and 4).

The lipids DEPC and DOPC also exhibit the same behavior. DOPC is an interesting case, however, as the liquid crystal state persists (under excess water conditions) down to −16°C, even though ice forms at about −12°C on cooling. Although this is in contrast to the results reported in Caffrey (1987), we note that those measurements correspond to a time-resolved diffraction experiment. Even more unusual is the hysteresis in the lattice constant within the gel phase (Fig. 6). Note that ice is present throughout the temperature range where this hysteresis is observed, which is not true for the other cases of hysteresis we observe. The reason for this behavior is under investigation.

CHEMICAL POTENTIAL MEASUREMENTS

Many researchers have studied the relationship between osmotic pressure difference and other observables such as water layer thickness in lamellar systems (Parsegian et al.,

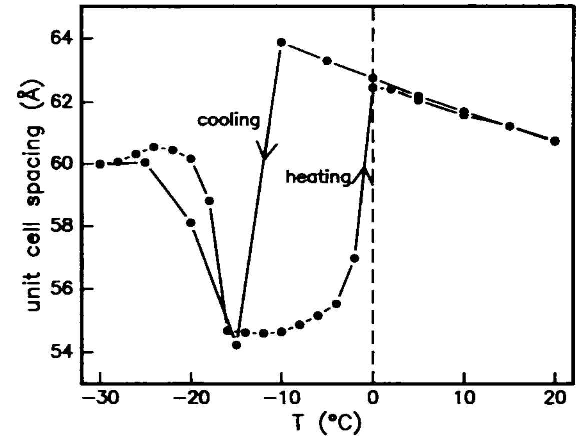

FIGURE 6 Unit cell spacing of DOPC in excess water as a function in temperature. Notice the hysteresis around −18°C. This is the L_α–L_β transition. It must be stressed that ice is present throughout the temperature interval of this hysteresis.

1979), water core diameter in hexagonal phase lipid systems (Gruner et al., 1986), functioning of both membrane (Zimmerberg and Parsegian, 1986) and globular (Colombo et al., 1992) proteins, and the distance between polysaccharides (Rau and Parsegian, 1990). Combining osmotic pressure difference measurements with microscopic structural information enables one to probe the net forces between macromolecules as well as to explore quantitatively the applicability of theoretical predictions for phenomena such as hydration repulsion and attraction, steric repulsion, and van der Waals attraction. Most studies of the variation of osmotic pressure difference with water layer thickness in lamellar systems focus on the hydration repulsion regime of layers separated by less than a few nanometers of water. When water is added to the interbilayer region, work is expended as the new water is ordered by the lipid headgroups. This results in an effective repulsion between neighboring lipid bilayers. Note that the contribution to the overall free energy from associating more water with the headgroups outweighs this work, so that the net change in free energy is negative. In this regime, the osmotic pressure of water incorporated into a lipid bilayer with thickness of the water layer d_f varies as

$$\pi = \pi_0 \exp\left(\frac{-d_f}{\lambda}\right) \qquad (2)$$

where π_0 is a scale factor, and λ is the hydration repulsion decay length. At lower osmotic pressures, beyond the range of hydration repulsion, this regime either gives way to electrostatic repulsion for charged species or van der Waals attraction for neutral molecules (Parsegian et al., 1986).

When water incorporated between bilayers freezes, it migrates out of the lamellar lattice, perhaps into interstitial regions where it forms pockets of ice. If we imagine that no water migration has taken place, i.e., that the water has frozen in place between the bilayers, for the bilayers to approach each other to the degree observed the ice would have to be very much denser than water; this is inconsistent with both the electron density reconstruction and the observation that the ice Bragg peaks are at the expected scattering angle of ordinary ice; thus, we conclude that ice does not exist between bilayers. Similar behavior has been reported before in montmorillonite clay (Anderson, 1967). These pockets of ice exist as pools of water in equilibrium with the water still contained between the bilayers, which has not frozen. This is realized on the heating branch, on which ice is present (cf. Fig. 2). The lattice spacing, *a*, depends strongly on a temperature below 0°C because the chemical potential of ice varies with temperature differently than that of bound water. When the temperature is changed, the water repartitions until the chemical potentials again balance. Because the chemical potential of bound water depends strongly on the thickness of the water layer between bilayers, the repartitioning is manifested as a change in unit cell spacing of the lamellar lattice. Fig. 7 shows the change in d_f, as obtained from electron density reconstruction of the unit cell, as a function of temperature during a heating scan. Electron density reconstruction was chosen to specifically separate any effects of chain tilt or headgroup packing on the lattice constant *a*. The reconstruction also reveals that, whereas d_f changes by almost a factor of three between −15°C and 0°C, the bilayer thickness also changes by about 1 Å in this interval.

Thus, we have a system in which we can observe the equilibrium partitioning of water between two states. Moreover, one of the states is ordinary ice, the thermodynamic properties of which are comprehensively tabulated. We can therefore infer the chemical potential of water as it migrates from the ice state to the bound state between bilayers. It is important to note that below 0°C, osmotic pressure difference is ill-defined. A more fundamental way of looking at the situation is to describe the hydration repulsion regime with a pressure *p*, driving the bilayers apart. Assuming that the work needed to change the bilayer separation d_f is the dominant contribution to the change in chemical potential of water $\Delta\mu$, (Strictly speaking, $\Delta\mu$ includes whatever work is involved in modifying the bilayer structure as water partitions into the lamellar structure. Therefore, measurements of this quantity alone cannot provide information about molecular forces outside the context of specific microscopic models.) we arrive at

$$\Delta\mu = \int_{d_{exc}}^{d_f} pA\,dz \qquad (3)$$

where *A* is the area of the bilayer/mole of water, and d_{exc} is the bilayer separation under excess water conditions, where the water between the bilayers is in equilibrium with pure water: as a fiducial point, we take pure water at its freezing point. The justification for neglecting the chemical potential's change with temperature at constant bilayer spacing is discussed in the appendix. Within the context of osmotic pressure, $\Delta\mu = \pi v$; using the hydration repulsion law, $\Delta\mu = \pi_0 v \exp(-d_f/\lambda)$, where *v* is the molar volume of water. In our situation, $\Delta\mu = \Delta\mu(T)$ is the difference in chemical

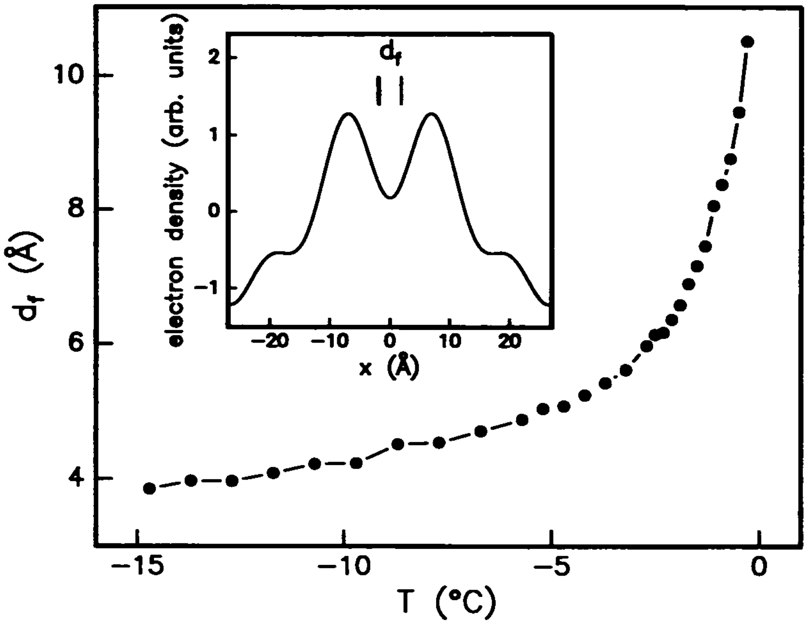

FIGURE 7 Water layer thickness d_f as a function of temperature (heating scan) for DOPC. This is obtained from the reconstruction inset. Following McIntosh et al. (1987), d_f is taken to be the distance between phosphorus maxima in the reconstruction minus 10Å. *Inset*: four-peak electron density reconstruction, using the phase set (+1, −1, −1, −1) of the unit cell of the lamellar lattice. x is a coordinate within the unit cell. d_f is indicated on the figure.

potential between water at its freezing point and ice at T. This is easily obtained using the equation of state for an ideal gas at vapor pressure p_v and T, where p_v is obtained using tables of the vapor pressure of ice (Hodgman, 1952). (We estimate the second virial coefficient of water vapor at 0°C to be less than 1% of the molar volume.) Specifically

$$\Delta\mu(T) = R(c+1)(T-T_t) - RT\log\left[\left(\frac{T}{T_t}\right)^{(c-1)}\frac{p_v}{p_t}\right]. \qquad (4)$$

Here, T_t and p_t are the temperature and vapor pressure at the freezing point: 273.15 K and 4.546 mm Hg. R is the gas constant, and $(c+1)R$ is the specific heat at constant pressure of water vapor, 36.1 J/mol/K. Let us specifically state our assumptions at this point. The change in chemical potential of water as the bilayer separation changes is dominated by hydration repulsion. As the temperature changes, the chemical potential of ice in equilibrium with this water changes in accordance with Eq. 4. We assume that changes in the lipid-water structure are such that the aforementioned chemical potentials are equal, which is the equilibrium condition when there are two populations of water molecules. The ice point not only represents a well-defined fiducial reference state, but also gives us self-consistency, because at the ice point the sample again recovers excess water conditions in which the chemical potential difference between interbilayer water and bulk water is 0; in terms of Eq. 3, $d_f = d_{exc}$. Thus a plot of the logarithm of $\Delta\mu(T)$ as given above versus d_f should yield both π_0 and λ. In contrast to the osmotic pressure difference methods of obtaining such a curve, we obtain this using only one temperature scan on one sample. Although this eliminates any errors caused by sample-to-sample variation, it is at the cost of being confined to subzero temperatures. Yan et al. (1993) have used deuterium nuclear magnetic resonance to measure the chemical potential of bound water in equilibrium with ice as a function of the amount of water frozen.

Fig. 8 shows the natural logarithm of $\Delta\mu$ of ice plotted against d_f for the phospholipid DEPC in excess water. The solid line indicates the straight line best fitting the data in the leftmost portion of the graph. This fit gives a λ value of 0.94 ± .02 Å. Note that at −40°C, $\Delta\mu$ is about 8 kJ/mol. To obtain this "hygroscopic stress" would require an osmotic pressure difference of more than 4×10^9 dyn/cm^2, which is much higher than can be easily achieved with standard methods (Parsegian et al., 1986). Notice that at lower $\Delta\mu$ the curve deviates from hydration repulsion; this deviation is thought to be the onset of van der Waals attraction between the bilayers counteracting the hydration repulsion.

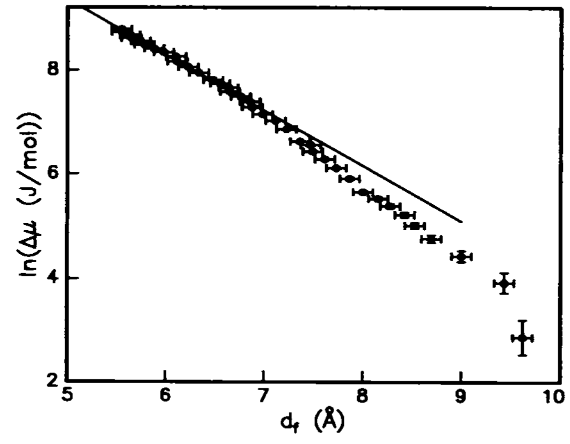

FIGURE 8 Natural logarithm of $\Delta\mu$ versus d_f for DEPC in excess water. The straight line indicates the hydration repulsion regime with $\lambda = 0.94 \pm .02$ Å. The drop below the straight line at lower $\Delta\mu$ is the crossover to the regime where hydration repulsion is balanced by attractive forces between bilayers.

Perhaps more interesting is a plot of the same quantities for DOPC in excess water (Fig. 9). Here, we also see the same exponential repulsion with a decay length of about 1.1 Å, but we also see at lower osmotic pressure another regime of exponential repulsion with decay length of 2.2 Å. Although it cannot yet be ruled out, it would be more than remarkable if this deviation from single exponential behavior were caused solely by either λ or π_0 varying with temperature in such a way as to cause the "knee" seen in Fig. 9; furthermore, similar behavior has previously been observed in another PC lipid using osmotic pressure difference methods (McIntosh et al., 1987). We note that a comparison between our measurements, which are necessarily conducted over a temperature range with room temperature osmotic stress measurements, is valid only if there are no phase transitions that alter significantly the elastic properties of the lipid tails. It must be pointed out that the most important difference between DOPC and DEPC in this temperature region is that DEPC is in the gel state below 10°C, whereas DOPC remains in the liquid-crystalline state down to −16°C.

What is most significant about Figs. 8 and 9 is not that λ is obtained with greater ease and considerably greater precision than with standard osmotic stress or vapor phase methods (Parsegian et al., 1986) but that the hydration repulsion is not well described by a single exponential. The deviation from a single exponential at $d_f \approx 7$ Å in Fig. 8 is both reproducible from sample to sample and well within the accuracy of the measurement. Given that d_f is inferred from the separation of phosphorus atoms in the unit cell reconstruction, it is conceivable that the extreme dehydration of the lamellar lattice at temperatures substantially below 0°C might alter the relationship between the separation of the phosphorus peaks and d_f. Using ice to measure the net hydration repulsion between macromolecules should be sufficiently precise to test quantitatively models of hydration forces that are more comprehensive than single exponential decays.

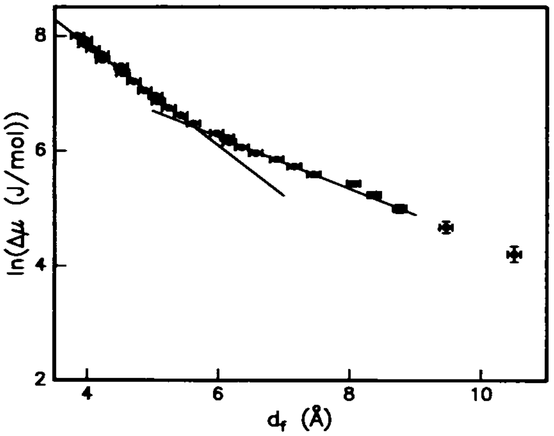

FIGURE 9 Natural logarithm of $\Delta\mu$ versus d_f for DOPC in excess water. The two lines are best fit straight lines. At higher $\Delta\mu$, the hydration repulsion decay length is 1.14 ± .04 Å; at lower $\Delta\mu$, a crossover is seen to a regime where $\lambda = 2.21 \pm .1$ Å.

CONCLUSION

Taken together, the observations listed above lead inescapably to one conclusion: crystalline ice does not exist between lipid bilayers in an ordered multilamellar phase in any of the systems studied. Although it cannot be proven, we have every reason to believe that this behavior is not specific to the lipids studied, but is generic. Fig. 3 demonstrates this phenomenon exceedingly well; when the lipid was prepared with 8.6 wt % water, in which case no diffraction from ice was observed, the lamellar lattice had a larger repeat spacing than even fully hydrated lipid, but only when ice was present in the latter sample. Moreover, lipid samples that were sufficiently hydrated for ice to form always exhibited the same lamellar lattice repeat spacing when ice was present, regardless of how much water was initially added. The observed hysteresis in temperature seen in Fig. 2 results because water was cooled below 0°C without any ice nucleated. DEPE hydrated with 8.6 wt % water can be cooled to at least −40°C without nucleating any ice, and it therefore remained on the metastable, supercooled water branch, exhibiting no hysteresis. This raises two issues. First, we expect that, were an ice crystal introduced into a sample while on the metastable branch, it would immediately jump to the lower, stable branch, and exhibit the same lattice constant as other samples in which ice has spontaneously formed. The other, more interesting issue is whether or not the water layer between lipid bilayers is so thin that it is sufficiently improbable to nucleate an ice crystal so that it never happens. We have held such a sample at −40°C for several days and never seen ice. This raises the possibility of physics somewhat more subtle than the equilibrium arguments that led to the Kelvin equation (Eq. 1); does the restriction of the water to such narrow confinement between very dehydrated lipid bilayers lead to a kinetic depression of the freezing transition, beyond what is expected from equilibrium considerations? In this sense "kinetic" means that in addition to the equilibrium freezing temperature, the barrier to nucleation may also be strongly affected by the confinement.

This paper contains two fundamental messages. First, studying water freezing in multilayers provides much the same information as more traditional osmotic methods, with greater precision, but also with the restriction to temperatures below 0°C. Second, water freezing immediately adjacent to bilayers is not well understood. The second message is arguably the more important. It is less obvious but nonetheless well established that much of the freezing damage in living cells results from the osmotic stress on their membranes that occurs when ice crystals in the cytosol cause highly concentrated solutions to stress the bilayer membrane. A better understanding of this process may lead, for example, to better ways to preserve foods or create winter-hardy plants.

We thank V. A. Parsegian, S. Leikin, O. Narayan, R. E. Goldstein, and M. W. Tate for insightful discussions.

This work was supported by the National Institutes of Health (grant

GM32614), the Department of Energy (grant DE-FG02-87ER60522), and the Office of Naval Research (contract N00014-91-J-1543).

APPENDIX

Because the bound water in the bilayer phase is in equilibrium with bulk ice, the chemical potential $\mu(T; a(T))$ for bound water is the same as that for ice. To interpret this within the context of hydration models, an additional assumption is needed. This purpose of this appendix is to explain the assumption clearly. The assumption in question is the equality of Eq. 3 to Eq. 4. We start with the identity

$$\begin{aligned}\mu(T; a(T)) - \mu(0^\circ\mathrm{C}; a(0^\circ\mathrm{C})) &= [\mu(0^\circ\mathrm{C}; a(T)) - \mu(0^\circ\mathrm{C}; a(0^\circ\mathrm{C}))] \\ &\quad + [\mu(T; a(T)) - \mu(0^\circ\mathrm{C}; a(T))].\end{aligned} \tag{A1}$$

Written in this manner, the first term is the work done because of the change in a in the presence of hydration repulsion. The second term is the difference in the chemical potential of water when the unit cell spacing is kept constant, but the temperature is changed. Explicitly stated, we have assumed the second term is negligible compared with the first term. It is possible to provide some justification for this assumption by comparing studies of the change in unit cell spacing of dilauroylphosphatidylcholine when equilibrated with dextran at 25°C, with temperature studies on lipids equilibrated with dextran, whose osmotic stress is known not to vary greatly with temperature (Parsegian et al., 1986). This justification is based on studies performed near room temperature. Whereas there is no reason to expect dramatically different behavior for lipids in the temperature range used in our study, the neglect of the second term in the equation above must be regarded only as an assumption that requires further experimental investigation.

REFERENCES

Anderson, D. M. 1967. The interface between ice and silicate surfaces. *J. Colloid Interface Sci.* 25:174–191.

Caffrey, M. 1987. The combined and separate effects of low temperature and freezing on membrane lipid mesomorphic phase behavior: relevance to cryobiology. *Biochim. Biophys. Acta.* 896:123–127.

Colombo, M. F., D. C. Rau, and V. A. Parsegian. 1992. Protein solvation in allosteric regulation: a water effect on hemoglobin. *Science.* 256: 655–659.

Doster, W., A. Bachleitner, R. Dunau, M. Hiebl, and E. Lüscher. 1986. Thermal properties of water in myoglobin crystals and solutions at subzero temperatures. *Biophys. J.* 50:213–219.

Gruner, S. M., J. R. Milch, and G. T. Reynolds. 1982. Slow-scan silicon-intensified target-TV x-ray detector for quantitative recording of weak x-ray images. *Rev. Sci. Instrum.* 53:1772–1778.

Gruner, S. M., V. A. Parsegian, and R. P. Rand. 1986. Directly measured deformation energy of phospholipid H_{II} hexagonal phases. *Faraday Discuss. Chem. Soc.* 81:29–37.

Gruner, S. M. 1989. CCD and vidicon x-ray detectors: theory and practice. *Rev. Sci. Instrum.* 60:1545–1551.

Hirsh, A. G., R. J. Williams and H. T. Meryman. 1985. A novel method of natural cryoprotection. *Plant Physiol.* 79:41–56.

Hodgman, C. D., editor. 1952. Handbook of Chemistry and Physics, 34th ed. CRC, Cleveland. 1952.

Knight, C. A., C. C. Cheng, and A. L. DeVries. 1991. Adsorption of α-helical antifreeze peptides on specific ice crystal surface planes. *Biophys. J.* 59:409–418.

Knight, C. A., and A. L. DeVries. 1989. Melting inhibition and superheating of ice by an antifreeze glycopeptide. *Science.* 245:505–507.

Kodama, M., H. Hashigami, and S. Seki. 1987. Role of water molecules in the subtransition of the L-dipalmitoylphosphatidylcholine-water system as studied by differential scanning calorimetry. *J. Colloid Interface Sci.* 117:497–504.

McIntosh, T. J., A. D. Magid, and S. A. Simon. 1987. Steric repulsion between phosphatidylcholine bilayers. *Biochemistry.* 26:7325–7332.

Milch, J. R. 1983. A focusing x-ray camera for recording low-angle diffraction from small specimens. *J. Appl. Cryst.* 16:198–203.

Narayan, O., P. T. C. So, D. C. Turner, S. M. Gruner, M. W. Tate, and E. Shyamsunder. 1990. Volume constriction in a lipid-water liquid crystal using high-pressure x-ray diffraction. *Phys. Rev. A.* 42:7479–7482.

Parsegian, V. A., N. Fuller, and R. P. Rand. 1979. Measured work of deformation and repulsion of lecithin bilayers. *Proc. Natl. Acad. Sci. USA.* 76:2750–2754.

Parsegian, V. A., R. P. Rand, N. L. Fuller, and D. C. Rau. 1986. Osmotic stress for the direct measurement of intermolecular forces. *Methods Enzymol.* 127:400–416.

Rau, D. C., and V. A. Parsegian. 1990. Direct measurement of forces between linear polysaccharides xanthan and schizophyllan. *Science.* 249: 1278–1281.

Rau, D. C., and V. A. Parsegian. 1992. Direct measurement of the intermolecular forces between counterion-condensed DNA double helices. *Biophys. J.* 61:246–259.

Singh, G. P., F. Parak, S. Hunklinger, and K. Dransfeld. 1981. Role of adsorbed water in the dynamics of metmyoglobin. *Phys. Rev. Lett.* 47: 685–688.

Yan, Z., J. Pope, and J. Wolfe. 1993. NMR of frozen phosphatidylcholine-D_2O suspensions: a new technique for measuring hydration forces. *J. Chem. Soc. Faraday Trans.* 89:2583.

Zimmerberg, J., and V. A. Parsegian. 1986. Polymer inaccessible volume changes during the opening and closing of a voltage-dependent ionic channel. *Nature Lond.* 323:36–39.